Inorg. Chem. **2007**, *46*, 3245–3250

Crystal-to-Crystal Oxidative Deprotonation of a Di(μ-hydroxo) to a Di(μ-oxo) Dimer of Dimolybdenum Units

F. Albert Cotton,[†,§] Zhong Li,[†] Carlos A. Murillo,*[,†] Xiaoping Wang,[†,‡] Rongmin Yu,[†] and Qinliang Zhao[†]

Department of Chemistry and Laboratory for Molecular Structure and Bonding, P.O. Box 3012, Texas A&M University, College Station, Texas 77842-3012

Received December 20, 2006

A crystal-to-crystal transformation of $(DAniF)_3Mo_2(\mu\text{-}OH)_2Mo_2(DAniF)_3$ (**1**) to $(DAniF)_3Mo_2(\mu\text{-}O)_2Mo_2(DAniF)_3$ (**2**), where DAniF is the anion (*p*-anisyl)NC(H)N(*p*-anisyl), by dioxygen provides rare insight into the deprotonation process effected by dioxygen. In this dimolybdenum system, the conversion occurs without significant loss of crystallinity. Although no intermediates have been directly observed, a compound containing the $[(DAniF)_3Mo_2(\mu\text{-}OH)(\mu\text{-}O)Mo_2(DAniF)_3]^+$ cation, a proposed intermediate, has been obtained independently. Possible pathways for the overall conversion of **1** to **2** are discussed.

Introduction

Solvent-free solid-state chemical reactions, although relatively uncommon, are of great interest, especially regarding the development of green chemistry.[1] The single-crystal-to-single-crystal (SCSC) solid-state transformation is an especially interesting category of such reactions, and it has been studied in a variety of organic reactions.[2] However, few examples of inorganic compounds have been discovered,[3] and most of them involve loss or change of solvent in the coordination sphere or networks, although a few redox reactions have also been reported.[3a,f,k,p]

Coupled deprotonation/electron loss processes, with the net effect of dehydrogenation, occur widely in organic, inorganic, organometallic, and biological chemistry.[4] Sometimes the two steps can be examined sequentially, but often they are concerted. When the agent effecting electron removal is elemental oxygen, formation of water is often a part of the process, as in eq 1.[5]

$$2H^+ + {}^1/_2O_2 + 2e \rightarrow H_2O \qquad (1)$$

Compounds of the types **I** and **II** in Scheme 1 were first reported in 1998,[6] where the formamidinate ligands employed were *N*,*N*′-di-*p*-tolylformamidinate. In that case, we found that the $(\mu\text{-}OH)_2$ compound was oxidized by atmospheric oxygen to the $(\mu\text{-}O)_2$ compound.

We recently reported[7] the series of transformations shown in Scheme 1 where again formation of H_2O according to eq

* To whom correspondence should be addressed. E-mail: murillo@tamu.edu.

† Texas A&M University.

‡ Present address: Department of Chemistry, P.O. Box 305070, University of North Texas, Denton, TX 76203.

§ Deceased, Feb 20, 2007.

(1) (a) Poliakoff, M.; Fizpatrick, J. M.; Farren, T. R. A.; Anastas, P. T. *Science* **2002**, *297*, 807. (b) Anastas, P. T.; Kirchtoff, M. M. *Acc. Chem. Res.* **2002**, *35*, 686. (c) Cheng, K.; Foxman, B. M.; Gersten, S. W. *Mol. Cryst. Liq. Cryst. Sci. Technol., Sect. A* **1979**, *52*, 77.

(2) (a) Toda, F. *Acc. Chem. Res.* **1995**, *28*, 480. (b) Tanaka, A.; Toda, F. *Chem. Rev.* **2000**, *100*, 1025. (c) Ohmori, O.; Kawano, M.; Fujita, M. *J. Am. Chem. Soc.* **2004**, *126*, 16292. (d) Turowska-Tyrk, I.; Trzop, E.; Scheffer, J. R.; Chen, S. *Acta Crystallogr.* **2006**, *B62*, 128. (e) Garcia-Garibay, M. A. *Acc. Chem. Res.* **2003**, *36*, 491.

(3) (a) Iorganidis, L.; Kanatzidis, M. G. *J. Am. Chem. Soc.* **2000**, *122*, 8319. (b) Chui, S. S.-Y.; Lo, S. M.-F.; Charmant, J. P. H.; Orpen, A. G.; Williams, I. D. *Science* **1999**, *283*, 1148. (c) Suh, M. P.; Ko, G. W. *J. Am. Chem. Soc.* **2002**, *124*, 10976. (d) Rather, B.; Zaworotko, M. J. *Chem. Commun.* **2003**, 830. (e) Lee, E. Y.; Suh, M. P. *Angew. Chem., Int. Ed.* **2004**, *43*, 2798. (f) Choi, H. J.; Suh, M. P. *J. Am. Chem. Soc.* **2004**, *126*, 15844. (g) Takamizawa, S.; Nakata, E.; Saito, T. *Angew. Chem., Int. Ed.* **2004**, *43*, 1368. (h) Halder, G. J.; Kepert, C. J. *J. Am. Chem. Soc.* **2005**, *127*, 7891. (i) Dieters, E.; Bulach, V.; Hosseini, M. W. *Chem. Commun.* **2005**, 3906. (j) Takaoka, K.; Kawano, M.; Tominaga, M.; Fujita, M. *Angew. Chem., Int. Ed.* **2005**, *44*, 2151. (k) Armentano, D.; Munno, G. D.; Mastropietro, T. F.; Julve, M.; Lloret, F. *J. Am. Chem. Soc.* **2005**, *127*, 10778. (l) Kondo, M.; Murata, M.; Nishihara, H.; Nishibori, E.; Aoyagi, S.; Yoshida, M.; Kinoshita, Y.; Sakata, M. *Angew. Chem., Int. Ed.* **2006**, *45*, 5461. (m) Di, L.; Foxman, B. M. *Chem. Mater.* **1992**, *4*, 258. (n) Vela, M. J.; Buchholz, V.; Enkelmann, V.; Snider, B. B.; Foxman, B. M. *Chem. Commun.* **2000**, 2225. (o) Sandor, R. B.; Foxman, B. M. *Tetrahedron* **2000**, *56*, 6805. (p) Iordanidis, L.; Kanatzidis, M. *Angew. Chem., Int. Ed.* **2000**, *39*, 1927. (q) Brezesinski, T.; Groenewolt, M.; Antonietti, M.; Smarsly, B. *Angew. Chem., Int. Ed.* **2006**, *45*, 781. (r) Papaefstathiou, G. S.; Zhong, Z.; Geng, L.; MacGillivray, L. R. *J. Am. Chem. Soc.* **2004**, *126*, 9158.

(4) (a) Ghisla, S.; Thorpe, C. *Eur. J. Biochem.* **2004**, *271*, 494. (b) Reetz, M. T.; Eibach, F. *Angew. Chem., Int. Ed. Engl.* **1978**, *17*, 278. (c) Bietti, M.; Capone, A. *J. Org. Chem.* **2006**, *71*, 5260.

10.1021/ic062443v CCC: $37.00 © 2007 American Chemical Society
Published on Web 03/17/2007

Scheme 1

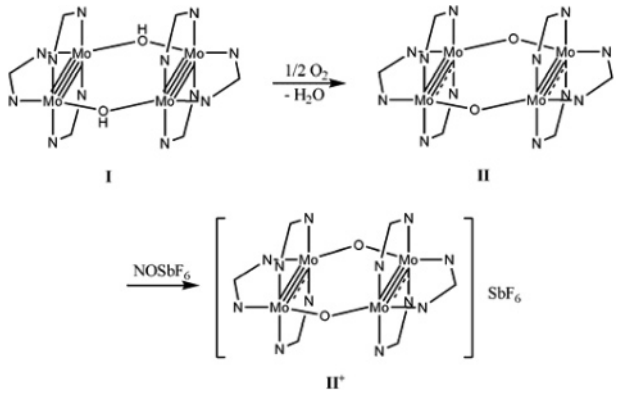

1 appears to accompany the conversion of **I** to **II**. In this case, the aryl groups in the bridging diarylformamidinate anions are *m*-$CF_3C_6H_4$. Independent of these two previously reported studies, we have also examined the oxidation of the homologous di(μ-OH) molecule in which the formamidinate ligands are the di-*p*-anisyl analogues. Even though this is the third such system to be studied, several results of nontrivial interest, that deepen our understanding of such reactions, were obtained, and they are presented here. We now report that the dimolybdenum molecular pair $Mo_2(DAniF)_3(\mu\text{-}OH)_2Mo_2(DAniF)_3$ (**1**) (DAniF = *N*,*N*′-di-*p*-anisylformamidinate) undergoes one oxidative conversion to a doubly oxidized product, $Mo_2(DAniF)_3(\mu\text{-}O)_2Mo_2(DAniF)_3$ (**2**), both in solution and as an SCSC process. We also have characterized a probable key intermediate with one OH and one O bridge.

Results and Discussion

Syntheses and Structural Results for 1 and 2. Compound **1** was synthesized from the reactions shown in eqs 2 and 3. The reaction of $Mo_2(DAniF)_3(OAc)$ and excess NaOMe leads to the formation of $Mo_2(DAniF)_3(OMe)(HOMe)$ (eq 2),[8] which was not isolated, but used in situ to react with H_2O (eq 3).

$$Mo_2(DAniF)_3(OAc) + NaOMe + MeOH \rightarrow Mo_2(DAniF)_3(OMe)(HOMe) + NaOAc \quad (2)$$

$$2Mo_2(DAniF)_3(OMe)(HOMe) + 2H_2O \rightarrow [Mo_2(DAniF)_3]_2(\mu\text{-}OH)_2 + 4MeOH \quad (3)$$

The yellow crystals of **1**·1.5CH_2Cl_2 used for X-ray work were obtained by placing a layer of isomeric hexanes over a CH_2Cl_2 solution. It crystallized in the space group $P\bar{1}$ with two independent molecules, each residing on an inversion center.[9] The molecular structure of **1** consists of two $Mo_2(DAniF)_3^+$ units which are linked by two hydroxide groups, as shown on the upper section of Figure 1.[10] For this crystalline form, the internal conformation of each Mo_2 unit is essentially eclipsed. The largest torsion angle about the Mo−Mo quadruple bond is 1.4(1)°. The crystallographically equivalent Mo−Mo distances of 2.1053(6) and 2.1058(6) Å shown in Table 1 are typical for a quadruply bonded Mo_2^{4+} unit with a $\sigma^2\pi^4\delta^2$ electronic configuration. The independent Mo−O distances in the range of 2.130(4) to 2.146(4) Å are close to those in similar molecular pairs with OH bridges.[7] The Mo−O−Mo angles are 144.6(2)° and 146.4(2)°. The nonbonding distance between the midpoints of the Mo−Mo bonds is about 4.09 Å.

Compound **1** reacts readily with either dry or atmospheric oxygen. Yellow crystals of **1** turn quickly to green on the surface and then to black. Long exposure to air produces a yet unidentified orange-brown, amorphous powder. When diamagnetic crystals of **1** are coated with mineral oil or Paratone oil to slow diffusion of air into the crystal and allowed to stand in air, there is a clean SCSC conversion.[11] The variations in metric dimensions that occur during such process over a period of 420 h are shown in Figure 2.[12] The Mo−Mo and Mo−O distances varied smoothly as oxygen was allowed to diffuse into the crystal. During this process the occupancy of the interstitial CH_2Cl_2 molecules significantly decreased,[13,14] as shown in Supporting Information, Table S1.

The total change in each of the metal-to-metal distances (0.045 Å) that occur during the SCSC process is consistent

(5) Some important processes for which this equation also applies are the C−H hydroxylation by cytochrome P450 (e.g.: Schöneboom, S.; Cohen, S.; Lin, H.; Shaik, S.; Thiel, W. *J. Am. Chem. Soc*. **2004**, *126*, 4017. Bathelt, C. M.; Zurek, J.; Mulholland, A. J.; Harvey, J. N. *J. Am. Chem. Soc*. **2005**, *127*, 12900.) and proton-coupled electron transfer from phenols, flavonols, and other antioxidants (e.g.: Sjödin, M.; Irebo, T.; Utas, J. E.; Lind, J.; Merényi, G.; Åkermark, B.; Hammarström, L. *J. Am. Chem. Soc*. **2006**, *128*, 13076. Fukumoto, L. R.; Mazza, G. *J. Agric. Food Chem*. **2000**, *48*, 3597).

(6) (a) Cotton, F. A.; Daniels, L. M.; Guimet, I.; Henning, R. W.; Jordan, G. T., IV; Lin, C.; Murillo, C. A.; Schultz, A. J. *J. Am. Chem. Soc*. **1998**, *120*, 12531. (b) Cotton, F. A.; Daniels, L. M.; Jordan, G. T., IV; Lin, C.; Murillo, C. A. *Inorg. Chem. Commun*. **1998**, 109.

(7) Cotton, F. A.; Murillo, C. A.; Yu, R.; Zhao, Q. *Inorg. Chem*. **2006**, *45*, 9046.

(8) (a) Cotton, F. A.; Liu, C. Y.; Murillo, C. A.; Villagrán, D.; Wang, X. *J. Am. Chem. Soc*. **2003**, *125*, 13564. (b) Cotton, F. A.; Liu, C. Y.; Murillo, C. A. *Inorg. Chem*. **2004**, *43*, 2267.

(9) On rare occasions, two different types of crystals were isolated from the same flask, both in the space group $P\bar{1}$ but differing in the number of interstitial CH_2Cl_2 molecules (**1**·1.5CH_2Cl_2 and **1**·CH_2Cl_2). In both cases the molecules of **1** are chemically the same. Crystal data for **1**·CH_2Cl_2: triclinic, $P\bar{1}$, a = 13.511(4) Å, b = 13.808(4) Å, c = 14.241(4) Å, α = 95.594(4)°, β = 109.780(5)°, γ = 107.869(5)°, V = 2318(1) Å^3, Z = 1, Mo(1)−Mo(2) = 2.1058(7) Å. Crystals of **1**·CH_2Cl_2 transform on exposure to air to **2**·CH_2Cl_2, also in SCSC fashion. Crystal data for **2**·CH_2Cl_2: triclinic, $P\bar{1}$, a = 13.486(3) Å, b = 13.741(3) Å, c = 14.255(3) Å, α = 95.435(4)°, β = 109.579(4)°, γ = 108.355(4)°, V = 2302.1(9) Å^3, Z = 1, Mo(1)−Mo(2) = 2.1540(6) Å.

(10) The bridging oxygen atoms are slightly disordered above and below the plane formed by the dimetal units and μ-O atoms. Similar disorder was observed in other formamidinate analogues; see refs 6a and 7.

(11) For comparison, yellow crystals of $[Mo_2(Dm CF_3F)_3]_2(\mu\text{-}OH)_2$ lost crystallinity immediately upon exposure to air; see ref 7.

(12) Data tables are provided as Supporting Information.

(13) In the limit of oxidation (when no CH_2Cl_2 was used in the refinement), calculations using PLATON/SQUEEZE show that the total potential solvent accessible void in **2** is 246 Å^3 and the electron count/cell is 32, which is much less than that expected (144 electrons/cell) for the three CH_2Cl_2 molecules that were present at the beginning of the process.

(14) Because of the loss of interstitial CH_2Cl_2 molecules, the mosaicity of the crystal of **2** increased and the *R* values are higher than those for **1**·1.5CH_2Cl_2. However, the bond distances for **2** are quite similar to those for the molecules in crystals of **2**·2CH_2Cl_2 that were obtained from solution.

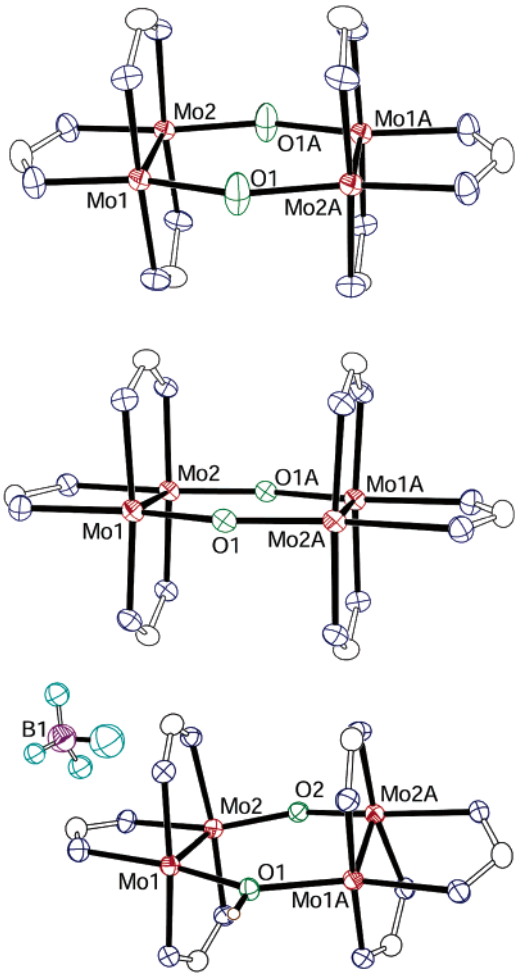

Figure 1. Core structures of compounds **1**·1.5CH_2Cl_2 (top), **2**·2CH_2Cl_2 (middle), and **3** (bottom) drawn with ellipsoids at the 40% probability level. Only one of the crystallographically independent molecules in **1**·1.5CH_2Cl_2 is shown. All *p*-anisyl groups and hydrogen atoms in the methine groups have been omitted for clarity.

Table 1. Selected Bond Lengths (Å) and Angles (deg)

compound	**1**·1.5CH_2Cl_2	**2**	**2**·2CH_2Cl_2	**3**
Mo(1)−Mo(2)	2.1053(6)	2.151(2)	2.1552(7)	2.1475(5)
Mo(3)−Mo(4)	2.1058(6)	2.151(2)		
Mo_2(1,2)···Mo_2(1A,2A)[a]	4.088	3.720	3.734	3.825
Mo_2(3,4)···Mo_2(3A,4A)	4.083	3.720		
Mo(1)−O(1)	2.146(4)	1.934(8)	1.933(2)	2.073(1)
Mo(2)−O(1)	2.145(4)	1.926(8)	1.935(2)	1.9174(8)[b]
Mo(3)−O(2)	2.130(4)	1.906(8)		
Mo(4)−O(2)	2.135(4)	1.939(8)		
Mo(1)−N(1)	2.170(4)	2.190(9)	2.191(2)	2.150(3)
Mo(1)−N(3)	2.131(4)	2.17(1)	2.174(2)	2.111(3)
Mo(1)−N(5)	2.166(4)	2.17(1)	2.176(2)	2.140(3)
Mo(2)−N(2)	2.152(4)	2.169(9)	2.152(2)	2.158(3)
Mo(2)−N(4)	2.121(4)	2.16(1)	2.191(2)	2.162(3)
Mo(2)−N(6)	2.155(4)	2.152(9)	2.130(2)	2.138(3)
Mo(3)−N(7)	2.156(4)	2.170(9)		
Mo(3)−N(9)	2.139(4)	2.18(1)		
Mo(3)−N(11)	2.149(4)	2.17(1)		
Mo(4)−N(8)	2.153(4)	2.17(1)		
Mo(4)−N(10)	2.122(4)	2.19(1)		
Mo(4)−N(12)	2.141(4)	2.15(1)		
Mo(1)−O(1)−Mo(2A)	144.6(2)	149.1(4)	149.70(9)	143.6(2)[c]
Mo(3)−O(2)−Mo(4A)	146.4(2)	150.8(4)		154.4(2)[d]

[a] Distance between the midpoint of the two [Mo_2] units. [b] Mo(2)−O(2). [c] Mo(1)−O(1)−Mo(1A). [d] Mo(2)−O(2)−Mo(2A).

with the final product having two Mo_2^{5+} species. The short Mo−O distances of 1.926[9] Å also support the formulation

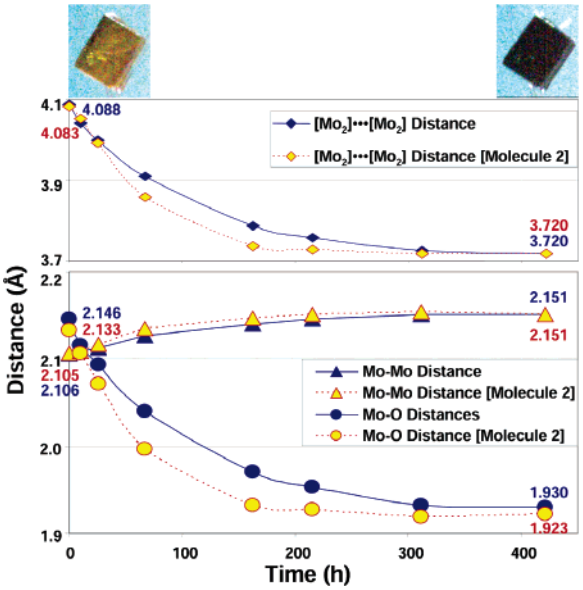

Figure 2. Changes in distances as oxidation from **1**·1.5CH_2Cl_2 to **2** takes place. Data were collected at 213 K. The time was obtained by adding the periods in which the crystal was exposed to air at ambient temperature between collections of data sets. In the upper part, the crystals are shown before (upper left) and after (upper right) exposure to air. There are two crystallographically independent molecules in the crystal, each on an inversion center.

of the bridging groups as oxo species. This formulation as $Mo_2(DAniF)_3(\mu\text{-}O)_2Mo_2(DAniF)_3$ (**2**) is unambiguous because this compound can also be prepared directly from **1** in solution by reaction with pure dioxygen or oxygen in air and crystallized as the solvate **2**·2CH_2Cl_2 (shown at the center of Figure 1), which has similar bond distances (Mo−Mo = 2.1552(7) Å and Mo−O = 1.934[3] Å). What is not unambiguous from the crystallographic data is whether there is an intermediate that formally has a Mo_2^{4+} and a Mo_2^{5+} species with one oxo and one hydroxo bridging group. Careful analyses of the data indicate that the data sets corresponding to the partially reacted crystals show only a single diffraction pattern, suggesting a one-phase topotactic reaction which could be consistent with the existence of an intermediate with one Mo_2^{5+} unit. It should be noted that such an intermediate would be expected to be paramagnetic. By analogy to other molecular pairs having one $(DAniF)_3Mo_2^{2+}$ unit, such species would be expected to be EPR active.[15] When EPR spectra were taken using solid samples of **1** exposed to small amounts of air, these were devoid of signals.[16] The lack of signals suggests that during the SCSC transformation **1** is oxidized to **2** without accumulation of intermediates in the crystal.

Solution Behavior. As indicated earlier, compound **2** can be made from **1** in solution by reaction with pure dioxygen or oxygen in air. When this transformation was followed

(15) See for example: (a) Cotton, F. A.; Liu, C. Y.; Murillo, C. A.; Villagrán, D.; Wang, X. *J. Am. Chem. Soc.* **2004**, *126*, 14822. (b) Cotton, F. A.; Liu, C. Y.; Murillo, C. A.; Zhao, Q. *Inorg. Chem.* **2006**, *45*, 9493. (c) Reference 7.

(16) Excess oxygen turned the color of the solid (and also solutions) to red. Because this mixture did not provide good crystalline samples, it has not yet been identified. In solution exposed to excess oxygen, the NMR and EPR spectra showed that the mixture contained paramagnetic species.

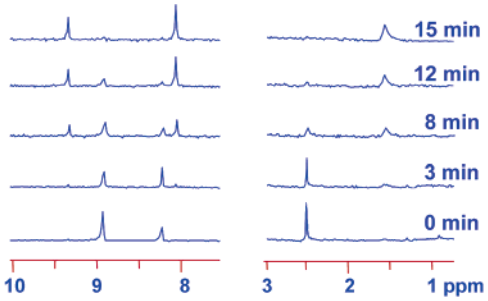

Figure 3. The methine and OH^-/H_2O regions of the ^1H NMR spectra as a CD_2Cl_2 solution of $[Mo_2(DAniF)_3]_2(\mu\text{-}OH)_2$ (**1**) is oxidized by O_2 to $[Mo_2(DAniF)_3]_2(\mu\text{-}O)_2$ (**2**) over a 15 min period.

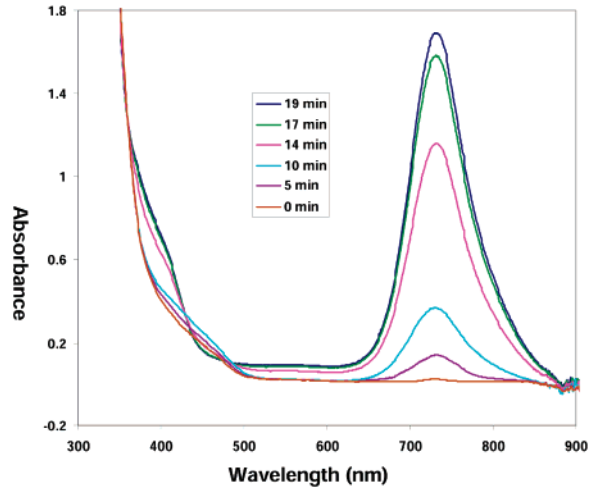

Figure 4. UV−vis spectra in CH_2Cl_2 solution showing the conversion of $[Mo_2(DAniF)_3]_2(\mu\text{-}OH)_2$ to $[Mo_2(DAniF)_3]_2(\mu\text{-}O)_2$. The color code for the time of exposure is given in the inset.

spectroscopically, two very important facts were learned from ^1H NMR spectroscopy: (1) There is no intermediate detectable by NMR. (2) As μ-OH groups disappear from the spectra, they are replaced by H_2O molecules. Figure 3 presents the spectra to support these statements; the spectra in the intermediate range of chemical shifts (which are not shown) are consistent with these conclusions but too complicated to allow detailed interpretation.[17] In the 8−10 ppm region it is clearly shown that the set of ligand methine signals for **1** (at 8.9 and 8.2 ppm, 2:1 ratio) disappear and are replaced by those for **2** (at 9.3 and 8.0 ppm, 1:2 ratio). In the 1−3 ppm region the OH signal at 2.4 ppm disappears while the H_2O signal at 1.6 ppm grows. In neither region is there any signal for an intermediate, such as a dimer with one μ-OH and one μ-O bridge. However, a neutral intermediate that has lost one H^+ and one electron (i.e., one species with a μ-OH and a μ-O) should give no sharp NMR spectrum, since it is paramagnetic, vide supra. On the other hand, if present only in very low concentration, it would also not affect the spectra of **1** and **2**.

The UV−vis spectra of a solution of **1** as it is being oxidized offer definite, though not quantitatively interpretable, evidence that there is a short-lived intermediate in the conversion of **1** to **2**. Figure 4 shows spectra over a 19 min period during which all of compound **1** in CH_2Cl_2 solution was oxidized to **2**. It must be clearly understood that these spectra do not constitute a kinetic study, because the rate of diffusion of oxygen into the solution was not uniform either in time or in space. In fact, the large change between the 10 min and the 14 min spectra is due to the fact that during this time interval the cap was removed from the sample container and the solution was agitated, thus introducing fresh dioxygen.

The important fact shown by these spectra in the 350−500 nm range is that there are more than two chromophores (i.e., not just **1** and **2**) present in the middle period of the overall oxidation process. The simplest explanation would be that there is one transient intermediate that absorbs in the 400−500 nm range. The probable identity of that intermediate (which, from its failure to show up in the ^1H NMR spectra, is presumed to be paramagnetic) will be discussed later.

Because the transformation of **1** to **2**, either in solution or in the solid state, requires the loss of four particles—two electrons and two protons—numerous pathways or sequences of steps (although not necessarily four discrete steps) are á priori possible. Thus, several different tetramolybdenum intermediates as well as some other intermediates (e.g., $OH^\bullet$, $O_2H^\bullet$) might occur, and presumably, at least one of each type occurs. To be rigorously accurate, we do not have firm evidence that H_2O rather than, perhaps, H_2O_2 is the other end product in the SCSC process, but we believe this to be by far the most logical presumption,[18] as indicated in the upper part of Scheme 1.

Since in the solid state the transformation of **1** to **2** occurs quantitatively and without significant loss of crystallinity,[19] it seems safe to assume that only an intermediate or intermediates, that have isosteric bridging groups, i.e., two μ-OH, one μ-OH and one μ-O, or two μ-O bridges, need be considered. Also, it seems reasonable to assume that, in the actual sequence, there will be neither two successive proton losses nor two successive electron losses. Thus, consideration may be accorded to only the sequences shown using the core structures in Scheme 2.

The intermediate **Y** would be accompanied by either $O_2H^\bullet$ or $OH^\bullet$.[20] The species **Y** would then be attacked to produce either of the next intermediates, $\mathbf{Z}^+$ (plus O_2H^- or OH^-) or $\mathbf{Z}^-$ (plus O_2H^+ or OH^+). Since the intermediacy of O_2H^+ or OH^+ seems very unlikely, we believe that the intermediate $\mathbf{Z}^-$ can be ruled out. It should also be noted that the sequence $\mathbf{1} \rightarrow \mathbf{X}^+ \rightarrow \mathbf{Y}$ would entail formation of O_2^- (the well-known superoxide ion), whereas the sequence $\mathbf{1} \rightarrow \mathbf{X}^- \rightarrow \mathbf{Y}$ would generate the intermediate O_2H^+, which seems very much less likely.

If **Y** is accompanied by $O_2H^\bullet$, the latter might not directly attack **Y** but be converted to $OH^\bullet + O_2$, with $OH^\bullet$ then attacking **Y** to give $\mathbf{Z}^+$ and OH^-.

(17) The complete spectra are available as Supporting Information.

(18) During refinement of crystal data for **2**, there was indication that an interstitial water molecule was present in the crystal.

(19) There is only a small loss of crystallinity due to loss of interstitial solvent as crystals were cooled on a stream of N_2.

(20) For a recent study of the reduction of O_2 to $O_2H^\bullet$, see: Geletti, Y. V.; Hill, C. L.; Atalla, R. H.; Weinstock, I. A. *J. Am. Chem. Soc.* **2006**, *128*, 17033−17042.

Scheme 2

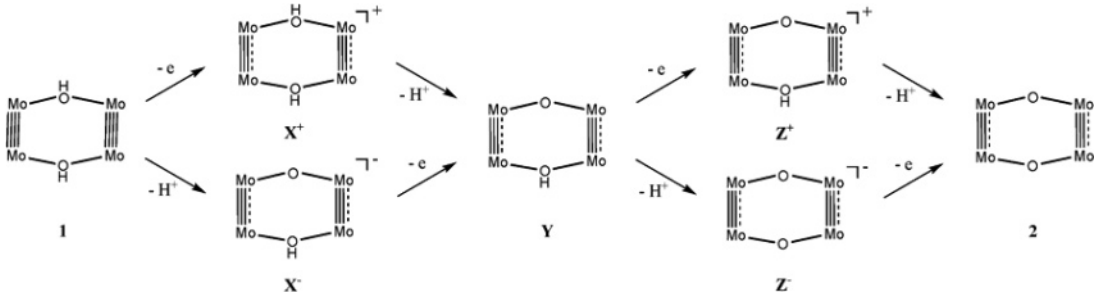

In any case, we suggest that the most likely sequence of tetramolybdenum intermediates in the conversion of **1** to **2** by O_2 is

$$\mathbf{1} \rightarrow \mathbf{X}^+ \rightarrow \mathbf{Y} \rightarrow \mathbf{Z}^+ \rightarrow \mathbf{2}$$

If the rate-determining step is $\mathbf{1} \rightarrow \mathbf{X}^+$ and this is much slower than the three steps that follow it, detection of $\mathbf{X}^+$, **Y**, or $\mathbf{Z}^+$ may be difficult. It is true that $\mathbf{X}^+$ and **Y** should each have an unpaired electron, but they do not accumulate as suggested by the absence of EPR signals.

Additionally, the proposed intermediate $\mathbf{Z}^+$ cannot be confirmed in situ while the oxidation of **1** to **2** is actually in progress because it is generated from **Y** simultaneously with OH^-, with which it immediately reacts to produce **2** and H_2O. However, in the absence of OH^-, $\mathbf{Z}^+$ should be stable, and its existence is strongly supported by the preparation of $\{[Mo_2(DAniF)_3]_2(\mu\text{-}O)(\mu\text{-}OH)\}BF_4$, **3**, by reaction of **2** with HBF_4 in CH_2Cl_2. This unsymmetrical compound and presumed intermediate in the deprotonation process crystallized in the space group *C*2/*c* with the tetranuclear cation having C_2 symmetry (bottom of Figure 1). The two Mo−Mo distances of 2.1475(5) Å are consistent with a bond order of 3.5, and they are close to those of 2.1552(7) Å in $[Mo_2(DAniF)_3]_2(\mu\text{-}O)_2$, in crystals of **2**·$2CH_2Cl_2$. The two sets of Mo−O distances, however, are distinctly different, with an average Mo−O(1) distance of 2.073(1) Å for the hydroxide bridged group and 1.9174(8) Å for Mo−O(2) in the oxide linker.

Conclusion

A dimolybdenum molecular pair, $Mo_2(DAniF)_3(\mu\text{-}OH)_2Mo_2(DAniF)_3$, was synthesized and studied by X-ray crystallography. The clean oxidative conversion of single crystals of **1** to $Mo_2(DAniF)_3(\mu\text{-}O)_2Mo_2(DAniF)_3$, **2**, has been observed and studied crystallographically in detail. These observations provide an interesting case of SCSC transformations and give a rare insight into the deprotonation process effected by dioxygen.

The overall reaction sequence, in schematic form is

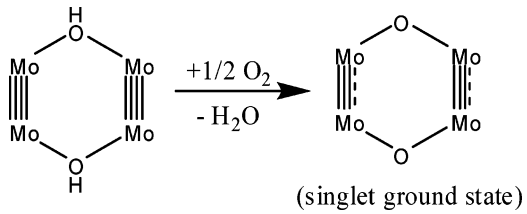

Experimental Section

Materials and Methods. Solvents were dried and then distilled under N_2 following conventional methods or purified under argon using a Glass Contour solvent purification system. Except where noted, synthetic operations were conducted under N_2 using Schlenk line techniques. The compounds $Mo_2(DAniF)_3(OAc)$[8,21] and HDAniF[22] were prepared by following published methods. Solutions of $(OEt_3)BF_4$ (1 M in CH_2Cl_2) and $NaOCH_3$ (0.5 M in methanol) were purchased from Aldrich and used as received.

Physical Measurements. Elemental analyses were performed by Robertson Microlit Laboratories, Madison, NJ. ^1H spectra were recorded on a Mercury-300 NMR spectrometer with chemical shifts (δ ppm) referred to residual solvent. Electronic spectra in the UV−vis range of 200−1000 nm were measured on a Shimadzu UV-2501PC spectrophotometer.

Preparation of $Mo_2(DAniF)_3(\mu\text{-}OH)_2Mo_2(DAniF)_3$ (1). A mixture of $Mo_2(DAniF)_3(OAc)$ (0.41 g, 0.40 mmol) in 20 mL of CH_2Cl_2 and 8 mL of 0.5 M NaOMe in methanol was stirred at ambient temperature for 1 h, leading to the formation of yellowish-orange supernatant solution with a suspended colorless NaOAc solid. After filtration, the filtrate was mixed with 0.10 mL of degassed H_2O. The mixture was layered carefully with 40 mL of isomeric hexanes. Sometimes two crystal forms (**1**·$1.5CH_2Cl_2$ and **1**·CH_2Cl_2) were obtained,[9] but usually only **1**·$1.5CH_2Cl_2$ was observed. The crystalline product was isolated by filtration, washed with 2 × 10 mL of hexanes, and then dried in vacuum. Typical yield: 0.25 g (63%). ^1H NMR (in CD_2Cl_2, ppm): 8.88 (s, 4H, N−C*H*−N), 8.19 (s, 2H, N−C*H*−N), 6.34 (d, 4H, aromatic), 6.22 (d, 8H, aromatic), ∼6.09−6.14 (m, 36H, aromatic), 3.61 (s, 24H, −OCH_3), 3.60 (s, 12H, −OCH_3), 2.42 (s, 2H, −O*H*). UV−vis in CH_2Cl_2, λ_{max} (nm) (ϵ, M^{-1} cm^{-1}): 449 (4.1×10^3). Anal. Calcd for $C_{90}H_{92}Mo_4N_{12}O_{14}$ (**1**): C, 55.45; H, 4.76; N, 8.62. Found: C, 55.64; H, 4.65; N, 8.33.

Preparation of $Mo_2(DAniF)_3(\mu\text{-}O)_2Mo_2(DAniF)_3$ (2). Crystals of **2** were obtained directly from crystals of **1**·$1.5CH_2Cl_2$ after exposure to air for 420 h.[23]

Preparation of $Mo_2(DAniF)_3(\mu\text{-}O)_2Mo_2(DAniF)_3$ (2·$2CH_2Cl_2$). A solution of **1** (0.24 g, 0.10 mmol) in 10 mL of CH_2Cl_2 was prepared under N_2. Air (10 mL) was then added to the Schlenk flask using a syringe. This mixture was stirred for 4 h, during which time the color of the solution changed from yellow to green. The product was essentially quantitatively precipitated by addition of hexanes. Single crystals of **2**·$2CH_2Cl_2$ were obtained by diffusion of isomeric hexanes into a dichloromethane solution. Yield: 0.19

(21) (a) Stephenson, T. A.; Bannister, E.; Wilkinson, G. *J. Chem. Soc.* **1964**, 2538. (b) Brignole, A. B.; Cotton, F. A. *Inorg. Synth.* **1972**, *13*, 87.
(22) Lin, C.; Protasiewicz, J. D.; Smith, E. T.; Ren, T. *Inorg. Chem.* **1996**, *35*, 6422.
(23) The yield is essentially quantitative, but the crystals changed to a paramagnetic, uncharacterized amorphous solid after being stored in air for about two months.

g (80%). ^{1}H NMR (in CD_2Cl_2, ppm): 9.31 (s, 2H, N−C*H*−N), 8.03 (s, 4H, N−C*H*−N), 6.40 (d, 8H, aromatic), ∼6.15−6.27 (m, 40H, aromatic), 3.63 (s, 12H, −OCH_3), 3.58(s, 24H, −OCH_3). UV−vis in CH_2Cl_2, λ_{max} (nm) (ϵ, M^{-1} cm^{-1}): 736 (2.0×10^4), 401 (1.9×10^3). Anal. Calcd for $C_{90}H_{90}N_{12}O_{14}Mo_4$ (**2**): C, 55.51; H, 4.66; N, 8.63. Found: C, 55.33; H, 4.45; N, 8.47.

Preparation of {[Mo$_2$(DAniF)$_3$]$_2$(μ-O)(μ-OH)}BF$_4$ (3). To a solution of $[Mo_2(DAniF)_3]_2(\mu\text{-}O)_2$ (30 mg, 0.015 mmol) in 10 mL of CH_2Cl_2 was added, with stirring, 1.5 mL of 0.01 M solution of HBF_4 in CH_2Cl_2.[24] The reaction mixture was stirred at room temperature for 2 h, and the color changed from green to brown. This solution was carefully layered with 30 mL of hexanes. Dark brown crystals formed after a period of 7 days. Yield: 20 mg (64%). ^{1}H NMR (in $CDCl_3$, ppm): 9.32 (s, 2H, N−C*H*−N), 8.02 (s, 4H, N−C*H*−N), 6.43 (d, 8H, aromatic), 6.25 (m, 24H, aromatic), 6.15 (d, 16H, aromatic), 3.67 (s, 12H, −OCH_3), 3.62 (s, 24H, −OCH_3), 2.20 (s, 1H, −O*H*). UV−vis in CH_2Cl_2, λ_{max} (nm) (ϵ, M^{-1} cm^{-1}): 550 (sh), 470 (3.8×10^3). Anal. Calcd for $C_{96}H_{105}BF_4Mo_4N_{12}O_{14}$ (**3**·C_6H_{14}): C, 54.35; H, 4.99; N, 7.92. Found: C, 55.24; H, 5.46; N, 8.39.

X-ray Structure Determinations. Single crystals of **1**·1.5CH_2Cl_2, **2**, **2**·2CH_2Cl_2, and **3** suitable for X-ray analyses were each mounted and centered on the tip of a cryoloop attached to a goniometer head. Data were collected at −60 °C on a Bruker SMART 1000 CCD area detector system. Cell parameters were determined using the program SMART.[25] Data reduction and integration were performed with the software package SAINT,[26] whereas absorption corrections were applied using the program SADABS.[27] The positions of the heavy atoms were found via direct methods using the program SHELXTL.[28] Subsequent cycles of least-squares refinement followed by difference-Fourier syntheses revealed the positions of the remaining non-hydrogen atoms. Hydrogen atoms were added in idealized positions. Non-hydrogen atoms, except some atoms from disordered groups and solvent molecules, were refined with anisotropic displacement parameters. Crystallographic data for **1**·1.5CH_2Cl_2, **2**, **2**·2CH_2Cl_2, and **3** are given in Table 2 and selected bond distances and angles in Table 1.

Table 2. X-ray Crystallographic Data

	compound			
	1·1.5CH_2Cl_2[a]	**2**	**2**·2CH_2Cl_2	**3**
formula	$C_{91.5}H_{93}Cl_3Mo_4N_{12}O_{14}$	$C_{90}H_{90}Mo_4N_{12}O_{14}$	$C_{92}H_{94}Cl_4Mo_4N_{12}O_{14}$	$C_{90}H_{91}BF_4Mo_4N_{12}O_{14}$
fw	2074.89	1947.50	2117.35	2035.32
space group	*P*$\bar{1}$ (No. 2)	*P*$\bar{1}$ (No. 2)	*P*$\bar{1}$ (No. 2)	*C*2/*c* (No. 15)
a (Å)	14.835(2)	14.736(3)	12.973(5)	24.683(3)
b (Å)	17.399(2)	17.278(4)	14.045(5)	14.138(2)
c (Å)	17.809(2)	17.590(4)	14.046(5)	26.693(3)
α (deg)	92.055(2)	91.605(4)	71.250(6)	90
β (deg)	88.116(2)	90.926(4)	73.612(6)	109.503(2)
γ (deg)	93.027(2)	96.177(4)	87.710(6)	90
V (Å^3)	4585.1(9)	4450(2)	2321(1)	8781(2)
Z	2	2	1	4
T (K)	213	213	213	213
d_{calcd} (g/cm^3)	1.503	1.453	1.515	1.540
μ (mm^{-1})	0.691	0.619	0.712	0.638
R1[b] (wR2)[c]	0.071 (0.159)	0.162 (0.261)	0.035 (0.072)	0.069 (0.116)

[a] The unit cell for **1**·1.5CH_2Cl_2 was transformed from a unit cell of the same compound with a conventional setting via the transformation matrix (−1 0 0 0 1 0 0 0 −1). The purpose of using an unconventional cell for **1**·1.5CH_2Cl_2 (see Table 1) is to facilitate the comparison of the results from time-dependent measurements. The β angle changed from 88.116(2)° in **1**·1.5CH_2Cl_2 to an obtuse angle (>90°) quickly and reached 90.926(4)° in **2** after 420 h. [b] $R1 = \Sigma||F_o| - |F_c||/\Sigma|F_o|$. [c] $wR2 = [\Sigma[w(F_o^2 - F_c^2)^2]/\Sigma[w(F_o^2)^2]]^{1/2}$.

Acknowledgment. We thank the Robert A. Welch Foundation and Texas A&M University for financial support.

Supporting Information Available: X-ray crystallographic data in standard CIF format for crystals of **1**·1.5CH_2Cl_2, **2**, **2**·2CH_2Cl_2, and **3**; CIFs also provided along with tables of X-ray crystallographic data, selected bond lengths (Å), and angles (deg.) as a single crystal **1**·1.5CH_2Cl_2 was oxidized by air to **2**; full ^{1}H NMR spectra collected at various intervals during the oxidation of [Mo$_2$(DAniF)$_3$]$_2$(μ-OH)$_2$ (**1**) to [Mo$_2$(DAniF)$_3$]$_2$(μ-O)$_2$ (**2**); cyclic voltammogram and differential potential voltammogram of [Mo$_2$(DAniF)$_3$]$_2$(μ-O)$_2$ (**2**). This material is available free of charge via the Internet at http://pubs.acs.org.

IC062443V

(24) The solution of HBF_4 in CH_2Cl_2 was made from a 0.5 mL volume of a 1 M solution of $(OEt_3)BF_4$ in CH_2Cl_2 which was diluted with CH_2Cl_2 to a volume of 50 mL. A trace amount of water was used to generate HBF_4.

(25) *SMART V 5.05 Software for the CCD Detector System*; Bruker Analytical X-ray System, Inc.: Madison, WI, 1998.

(26) *SAINT: Data Reduction Software*, V6.36A; Bruker Analytical X-ray System, Inc.: Madison, WI, 2002.

(27) *SADABS: Bruker/Siemens Area Detector Absorption and Other Corrections.* V2.03; Bruker Analytical X-ray System, Inc.: Madison, WI, 2002.

(28) Sheldrick, G. M. *SHELXTL*, V6.12; Bruker Analytical X-ray Systems, Inc.: Madison, WI, 2000.